

Thesis  
Engin.  
P37

# UNIVERSITY OF SASKATCHEWAN

This volume is the property of the University of Saskatchewan, and the literary rights of the author and of the University must be respected. If the reader obtains any assistance from this volume, he must give proper credit in his own work.

This Thesis by .....ERIK.C..B..PEDERSON.....  
has been used by the following persons, whose signatures attest their acceptance of the above restrictions.

---

*Name and Address*

*Date*

BETATRON ENERGY CONTROL

A

THESIS

submitted to

THE FACULTY OF ENGINEERING

in partial fulfilment of

the requirements for

THE DEGREE OF BACHELOR OF SCIENCE

in

ENGINEERING PHYSICS

UNIVERSITY OF SASKATCHEWAN

by

Erik Constantino Bernardo Pederson



127688

Saskatoon, Saskatchewan

April, 1955

## Acknowledgments

I would like to thank Dr. L. Katz for his help in the project described in this thesis. This work was made possible through the financial assistance of the National Research Council.

---

## Introduction

The Allis-Chalmers betatron is a high-energy induction electron accelerator commercially made for taking industrial X-ray photographs. In this application, the electrons emitted from a hot filament are accelerated during the first quarter-cycle of an alternating magnetic field, which is excited by a 180 cps sine wave source. During the acceleration, the electrons are constrained to a stable orbit of constant radius by having the field of special shape. When the electrons have reached the desired energy, the orbit is expanded and the electrons strike a thin, heavy-element target. The rapid deceleration causes the electrons to lose their energy principally in the form of gamma rays (X-rays). The energy spectrum of these rays is continuous and ranges up to the kinetic energy of the electrons when they strike the target.

In nuclear physics work, the maximum energy of the X-ray spectrum must be accurately known and continuously variable. This means that the orbit must be expanded at the time in the cycle when the electrons have the required energy. This present work is concerned with the electronic circuitry which has been developed to cause the orbit to expand when the instantaneous electron energy



reaches some adjustable, preset value.

### Determination of Instantaneous Electron Energy

From one of Maxwell's equations, we find that for the betatron electron orbit, the change in electron energy  $dE$  per revolution is proportional to the time rate of change of the total flux  $\frac{d\phi}{dt}$  linking the orbit. The energy  $E$  of the electrons will then be proportional to  $\int_0^\phi d\phi = \phi$  because the electrons are accelerated from rest at zero flux. The flux  $\phi$  is a function of the instantaneous magnet current  $I$ . This function would be linear if the permeability of all parts of the magnetic circuit were constant, since the total flux linking the orbit is given by  $\phi = BA$ , where  $B$  is the average flux density and  $A$  is the area of the orbit which remains constant. With constant permeability, the shape of the field would remain constant throughout the cycle. The permeability actually varies, however, since the wafer and sharp edges of the pole pieces approach saturation when the magnetizing current  $I$  is at its maximum. This current could be measured directly to determine the time to cause orbit expansion, but it is easier to use one of the following

methods.

The first method makes use of the voltage which appears across the magnet excitation winding. If this voltage is integrated with respect to time, it will closely represent the instantaneous electron energy, since the impedance presented to the exciting current  $I$  is almost purely inductive. The field excitation winding on the magnet has a center tap at ground potential. About 8000 volts rms appears across one half of this winding when the magnet is operated at 24 Mev.

The second method makes use of the voltage induced by the changing flux in a pickup coil of 14 turns wound around the wafer and located about the plane of the electron orbit (see Fig. 6). The peak voltage across this coil is 1400 volts at a magnet excitation energy of 24 Mev. The use of a separate pickup coil to obtain the voltage for the integrator has certain advantages over using the voltage appearing across the magnet excitation winding. The field at the pickup coil is very closely representative of the field that the electron beam experiences, since the pickup coil is located close to the electron orbit and the field shape does not vary significantly with time. This method is relatively insensitive to saturation effects in the magnetic circuit. The second

method is in use in the NRC betatron at the University of Saskatchewan at the time of writing this thesis and gives very satisfactory performance.

With either method, the voltage must be integrated with respect to time to obtain a new voltage which is proportional to the instantaneous electron energy. This is done with an integrating circuit.

### The Integrating Circuit

The circuit previously in use was a simple RC integrating circuit, which integrated the 8000 volts rms signal appearing across the magnet excitation winding to give a 90 volt peak output voltage. Now, however, the signal for the integrating circuit is obtained from the separate pickup coil described above, and the integrating circuit has been improved by adding an air-core inductance in series with the resistance (see Fig. 6). The largest voltage which would appear across the pickup coil was limited by insulation problems to about 2000 volts. Analysis then showed that the use of this inductance in the integrator gave better integration with the lower input voltage of 1400 volts peak than the simple RC integrator

gave with an input voltage of 8000 volts rms. Here, the integrator output voltage is the same (90 volts peak) for both integrators, at 24 Mev. magnet excitation energy.

The analysis (given in the appendix) of the LRC integrator using the pickup coil shows it to be almost completely independent of line frequency changes. The circuit is directly dependent on changes in C and in R; that is,  $\frac{dE}{E} = \frac{dC}{C}$  for changes in capacity, and  $\frac{dE}{E} = \frac{dR}{R}$  for changes in resistance. The dependences of E on L,  $\omega$ ,  $\theta$  and  $\tau$  are shown in Fig. 5. The time  $\tau$  is defined to be the delay between the time the voltage comparison circuit puts out its pulse and the time that the electron beam actually strikes the target. This is due to the finite response time of the thyatron (type FG105) and ignitron (type GL415) in the expander circuit. Since the electron energy changes most rapidly at the beginning of the acceleration period, this delay, if not constant, will give most trouble at low X-ray energies.

#### Requirements of the Voltage Comparison Circuit

This circuit had to be stable over long periods of time and be insensitive to power supply fluctuations. It

was decided to aim for a stability of  $\pm 2$  kev over the whole range up to 24 Mev. With such stability it would be possible to detect some of the weaker nuclear levels which have been previously beyond the reach of betatron stability. A slow drift of a few kev per day would be tolerated, since it could be measured and allowed for.

It was felt desirable to keep the energy jitter down to a few kev, although Penfold (private communication) has shown that a jitter of  $\pm 20$  kev in maximum energy would not obscure most of the sought-after levels. The existence of any spread in energy may be detected by observing the sharpness of the threshold in the activation curve of  $\text{Cu}^{63}$ . The  $\text{Cu}^{63} (\gamma, n)$  reaction has an especially sharp threshold, and this was used to test for energy jitter in the completed circuit.

A minimum energy increment of about 1 kev was desired, and it was found that a stock 50 K Helipot with a minimum resistance increment of 1.32 ohms was available. This gave a minimum energy increment of 0.7 kev. A mechanical slow-motion screw was built onto the Helipot to enable settings to be reproducibly made.

The output pulse was required to be greater than 50 volts from a low impedance output circuit, with a rise of greater than 30 volts per microsecond. This was necessary

to trigger the following multivibrator with certainty and with the minimum of time jitter.

### Circuit Description

The circuit finally arrived at (see Fig. 1) is a modification of the "Multiar" (which is described in M.I.T. Radiation Laboratory Series, Waveforms, McGraw-Hill, New York, 1949). The circuit employs regeneration, with the voltage comparison diode in the regeneration loop. The input cathode follower stage and the diode are compensated for cathode drift, which appears as a variable potential in series with the cathode. This potential is a strong function of heater voltage and also varies with tube age. Drift may be reduced from 100 millivolts per 10% change in heater voltage by a factor of 5 or 10 by balancing the drift of one half-section of a tube against the drift of the other half-section. The cathode drift in the input cathode follower stage is compensated by using one section of the twin triode as a diode-connected triode in series with the grid of the cathode follower section. Since the gain of the cathode follower stage is very nearly one, the compensation will be accurate. The cathode

drift in the voltage comparison diode is compensated by shunting the 100 K diode load resistor with an identical diode. Both diodes are in a single envelope, tube type 6AL5.

The circuit operates on the negative-going part of the negative half cycle of signal voltage. The signal voltage from the integrator is closely a sine wave of about 90 volts peak amplitude. The voltage comparator must not draw any appreciable current from the integrator, and therefore a cathode follower stage is used to isolate the voltage comparison diode from the integrator. The circuit and power supply are isolated from the chassis in order that certain advantages may be gained which would not be possible if the circuit ground were connected to chassis ground (betatron ground). The advantages will be seen from the following discussion of circuit operation.

A variable fraction of the reference voltage is tapped off the Helipot and appears between chassis ground (betatron ground) and circuit ground. With respect to circuit ground, this fraction is superimposed on the signal voltage as a variable dc component. The voltage comparison diode always starts to conduct when the cathode voltage drops to a certain value with respect to circuit ground. The part of the cycle where the diode conduction

starts is determined by the Helipot setting, but the voltage with respect to circuit ground at which diode conduction starts is always constant (except possibly for cathode drift). Thus, the voltage scale is independent of nonlinearity in the cathode follower, since for all Helipot settings the diode conduction starts at always the same point in the operating curve of the tube. It is also seen that the impedance in series with the diode is constant in this circuit, whereas if the diode were biased with a variable voltage as in conventional circuits, this impedance would not be constant and effective compensation for cathode drift could not be obtained over the whole energy range. These are the advantages which favor the choice of the floating ground type of circuit.

The pentode is biased to conduct heavily. When the voltage comparison diode begins to conduct, the feedback path through the pulse transformer in the pentode plate reinforces the dropping voltage on the diode cathode, and the pentode is rapidly cut off. The pulse is fed from the pulse transformer in the pentode cathode circuit into the output cathode follower. The output pulse is taken from the cathode follower pulse transformer and is fed to the next chassis through pin jacks. Crystal diodes (type 1N34) were placed across the windings of the pulse transformer



to eliminate ringing and multiple pulsing. A diode (type 6AL5) was placed across the output pulse transformer to eliminate ringing in the output pulse.

The reference voltage is monitored by comparing it with a pair of standard cells. The voltage divider is a physically large 50 K wirewound resistor with a small winding of the same kind of wire around the outside of the resistor to serve as the low resistance branch of the dividing chain. This arrangement makes the division ratio very nearly independent of temperature. A Leeds-Northrup current galvanometer gives a deflection proportional to the voltage difference between the tap on the divider and the standard cells. The cells are kept in a beaker of oil inside a Styrofoam box to reduce temperature variations. See Fig. 2.

The plate of the voltage comparison diode must be biased positively with respect to circuit ground, since when the input cathode follower grid is at circuit ground potential (corresponding to zero energy), the cathode is about 9 volts positive. Sufficient biasing on the diode plate extends the scale to zero energy. This bias voltage is obtained from the reference voltage by using a voltage divider. Wirewound resistors of the same type are bound together with the resistor on the low side of the tap

physically surrounded by the others. This arrangement makes the division ratio less sensitive to temperature variations.

Any remaining cathode drift may be detected by setting the Helipot to zero energy, then shorting the input to chassis ground (by pressing the lucite push switch on the panel) and unshorting the microammeter in series with the diode plate load resistor (by pressing the black push switch on the panel). Drift shows as a change in the microammeter reading.

The reference voltage is obtained across a type RCA 5651 voltage reference tube. This is a specially designed cold cathode type which gives good long-term stability (0.1 volt) and can be expected to give better stability than this when used under constant load as in this circuit. The tube is somewhat light sensitive and is shielded against light in this circuit. A 100 ohm potentiometer in series with the reference tube allows adjustments of the reference voltage to be made.

Another voltage divider on a different chassis allows the galvanometer and standard cells to check the supply voltage from the Lambda supply. A 150 ohm rheostat in series with the B+ lead allows adjustments to be made in the voltage supplied to the voltage comparator chassis. The

sensitivity of the monitoring circuit is such that a change in the Lambda supply voltage of 0.01 volt deflects the galvanometer 1 millimeter. A double-throw switch allows monitoring of either the Lambda supply or the reference voltage (see Fig. 2).

### Performance of System

The stability of the betatron was tested by counting the activity in samples of oxygen (in boric acid  $\text{H}_3\text{BO}_3$ ) which had been irradiated in the X-ray beam of the betatron. The samples were irradiated at an energy at which the activation curve had the largest fractional slope. Here, the statistical error is  $\frac{1}{2}\%$  and the fractional slope is 5% per 20 kev. This slope permits an energy shift of 2 kev to be detected. The stability for a series of irradiations is shown in Fig. 4. Here it is seen that about 30 minutes is required for the energy to drift down to a nearly constant value from the time of the beginning of a series of irradiations. The cause of this initial drift is not known. By interspersing a series of experimental irradiations on a sample with energy-monitoring irradiations on oxygen samples, the energy during

an irradiation may be interpolated. The highest short-term stability observed was an energy drift of 2 kev in a period of 1 hour.

---

## Appendix

Following is an analysis of the dependences of the peak energy  $E$  of the X-ray beam on various parameters, using the 14 turn pickup coil and the LRC integrator (Fig. 6).

We write  $\phi = \phi_0 \sin \omega t$ , where  $\phi$  is the instantaneous flux linking the electron orbit.

The electrons in the orbit have an instantaneous kinetic energy  $E^1 = E_0 \sin \omega t$   
 $= k_1 \phi_0 \sin \omega t$ .

The voltage induced in the pickup coil is

$$V = -k_2 \frac{d\phi}{dt} = -k_2 \omega \phi_0 \cos \omega t$$

$$= V_0 \cos \omega t$$

Now for the LRC circuit,

$$LC \frac{d^2 e}{dt^2} + RC \frac{de}{dt} + e = V$$

Now let  $V = \text{Real } (V_0 e^{j\omega t})$

$e = \text{Real } (\underline{e} e^{j\omega t})$ ,  $\underline{e}$  complex,

so that

$$-LC\omega^2 \underline{e} + j\omega RC \underline{e} + \underline{e} = V_0.$$

Solving, we obtain

$$\underline{e} = \frac{V_o}{(1 + \omega^2 LC)^2 + (\omega RC)^2} [1 - \omega^2 LC - j\omega RC]$$

and  $e = \text{Real} (\underline{e} e^{j\omega t})$

$$= \frac{V_o}{\sqrt{(1 + \omega^2 LC)^2 + (\omega RC)^2}} \left[ \frac{1 - \omega^2 LC}{\sqrt{(1 + \omega^2 LC)^2 + (\omega RC)^2}} \cos \omega t + \frac{\omega RC}{\sqrt{(1 + \omega^2 LC)^2 + (\omega RC)^2}} \sin \omega t \right]$$

Now let

$$\sin \theta = \frac{1 - \omega^2 LC}{\sqrt{(1 + \omega^2 LC)^2 + (\omega RC)^2}},$$

$$\cos \theta = \frac{\omega RC}{\sqrt{(1 + \omega^2 LC)^2 + (\omega RC)^2}},$$

$$\tan \theta = \frac{1 - \omega^2 LC}{\omega RC} \approx \theta$$

so that

$$e = \frac{V_o}{\omega RC \sqrt{1 + \theta^2}} \sin (\omega t + \theta)$$

Now to allow for any time delay  $\tau$  between the time the voltage comparison circuit puts out a pulse and the

time that the electron beam strikes the target, we write the energy of the X-ray beam  $E$  as

$$E = E_0 \sin \omega (t + \tau).$$

Thus we find

$$\begin{aligned} \frac{e}{E} &= \frac{V_0/E_0}{\omega RC \sqrt{1 + \theta^2}} \frac{\sin (\omega t + \theta)}{\sin (\omega t + \omega \tau)} \\ &= \frac{k_3}{RC \sqrt{1 + \theta^2}} \frac{\sin (\omega t + \theta)}{\sin (\omega t + \omega \tau)}. \end{aligned}$$

Now the peak value of  $e$  is to be 90 volts for the voltage comparator circuit. We choose  $C = 0.5 \times 10^{-6}$  farad. Then with  $\omega = 1130$  radians/second and  $\theta = 0$ , we find  $R = 3.1 \times 10^4$  ohms, and  $L = 1.56$  Henry. Also, with  $E_0 = 25$  Mev., we find  $k_3 = 0.05$ .

Now to a second order approximation,

$$\frac{\sin (\omega t + \theta)}{\sin (\omega t + \omega \tau)} = 1 - \frac{\theta^2}{2} + (\theta - \omega \tau) \cot (\omega t).$$

Thus

$$\frac{e}{E} = \frac{0.05}{RC \sqrt{1 + \theta^2}} \left[ 1 - \frac{\theta^2}{2} + (\theta - \omega \tau) \cot \omega t \right]$$

Now  $E = E_0 \sin \omega t$ , so  $\cos \omega t = \sqrt{1 - E^2/E_0^2}$ , and

$$\cot \omega t = \sqrt{\frac{E_0^2}{E^2} - 1}.$$

If we define  $A = \frac{RC \sqrt{1 + \theta^2}}{0.05} e$ , then it may be shown that

$$E = (1 - \frac{\theta^2}{2}) A - (\theta - \omega\tau) \sqrt{E_0^2 - A^2},$$

with  $\theta = \frac{1 - \omega^2 LC}{\omega RC}$  as before.

We may differentiate this expression for  $E$  to obtain the dependence of  $E$  on the parameters  $\omega$ ,  $L$ ,  $C$ ,  $R$ ,  $\tau$ ,  $E_0$ . The results are

$$\frac{dE}{dE_0} = \frac{-(\theta - \omega\tau)E_0}{\sqrt{E_0^2 - A^2}}$$

$$\frac{dE}{d\omega} = (\sqrt{E_0^2 - A^2} - \theta A) \left( \frac{L}{R} + \frac{1}{\omega^2 RC} \right)$$

$$\frac{dE}{dL} = -(\sqrt{E_0^2 - A^2} - \theta A) \frac{\omega}{R}$$

$$\frac{dE}{E} \approx \frac{dC}{C}$$

$$\frac{dE}{E} \approx \frac{dR}{R}$$

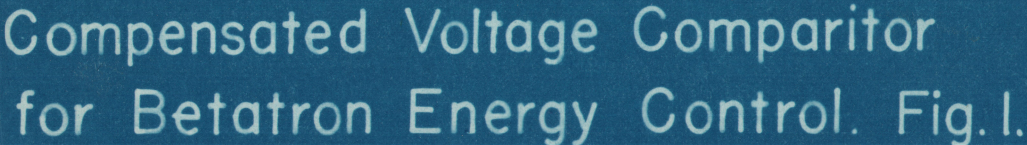
$$\frac{dE}{d\tau} = \omega \sqrt{E_0^2 - A^2}$$



The most important of these dependences are  $\frac{dE}{dE_0}$  (when  $\theta \neq 0$ ) and  $\frac{dE}{d\tau}$ . Some of these dependences are plotted in Fig. 5.

---





ECB Pederson 1955



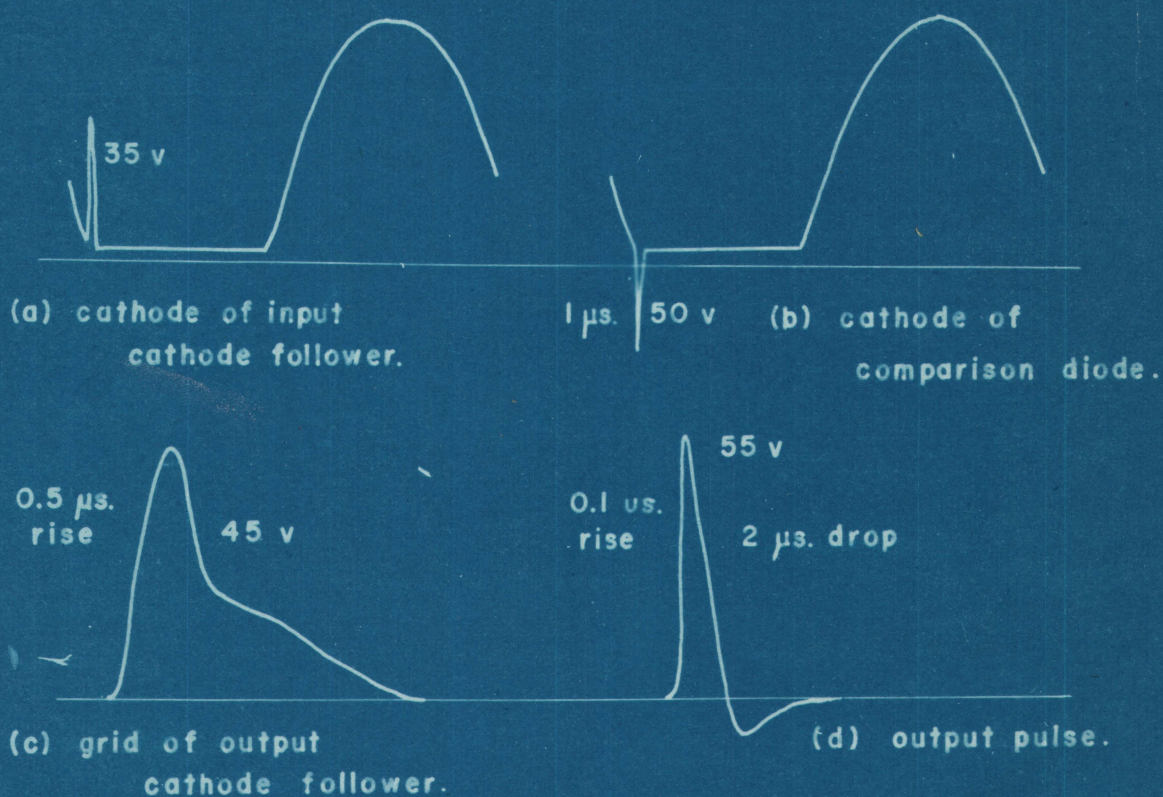
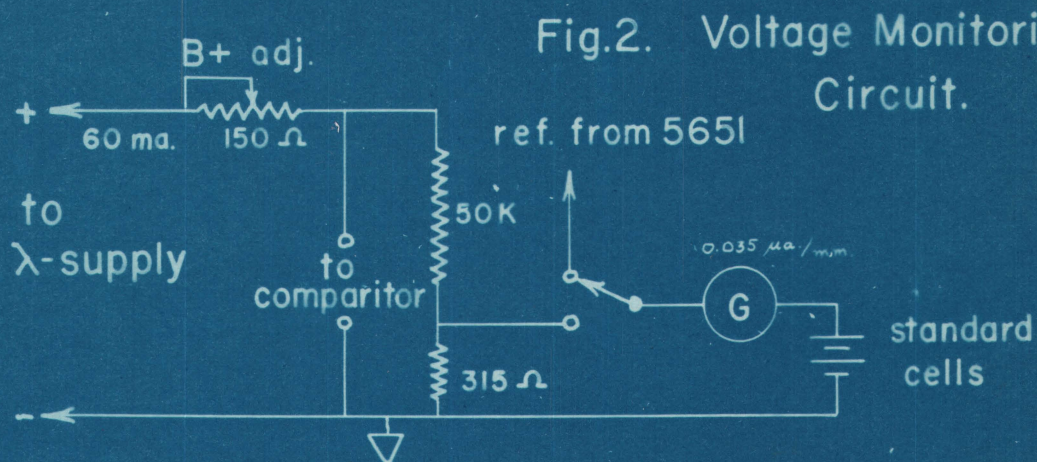
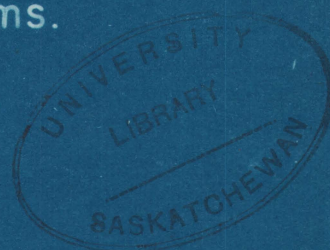
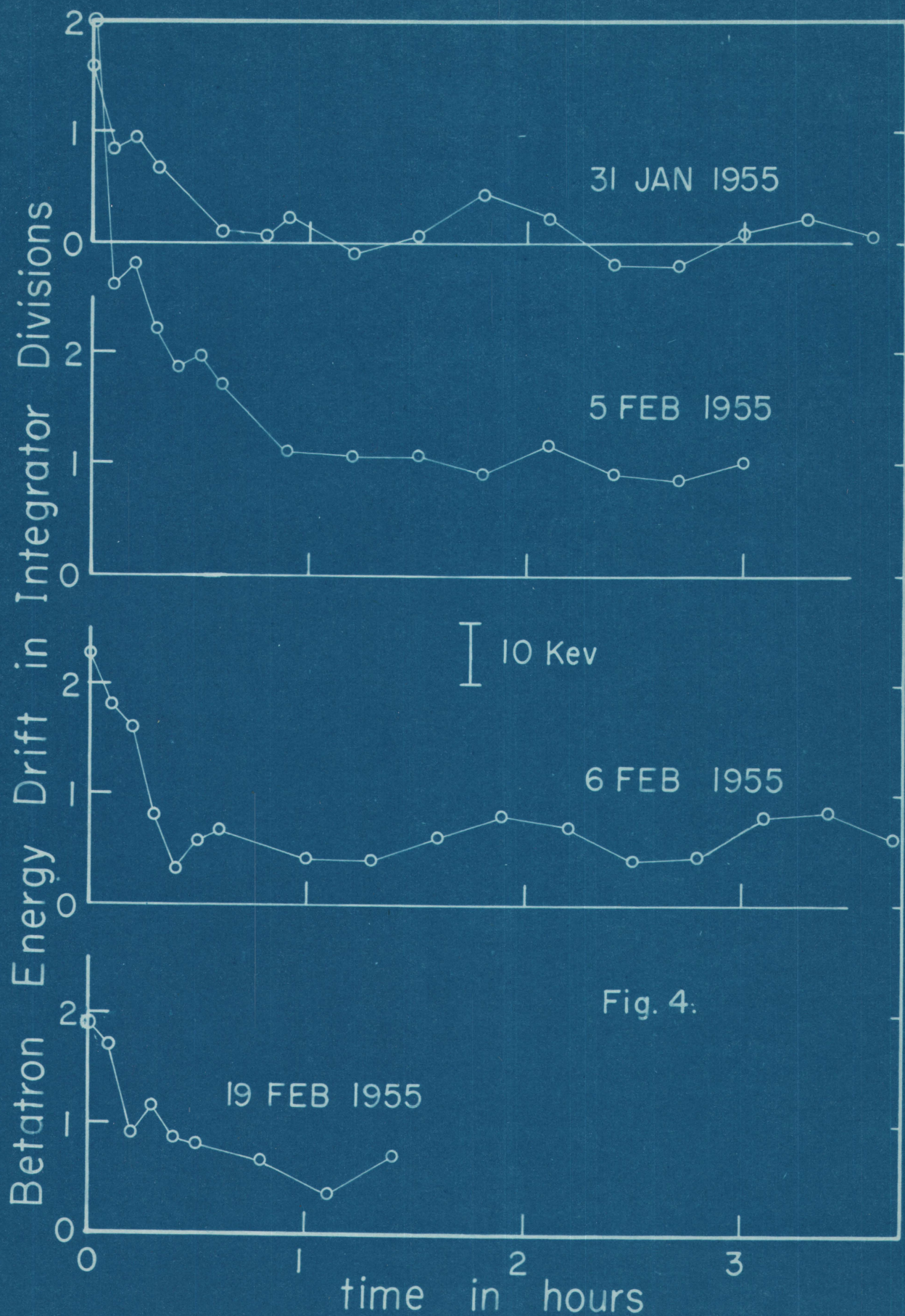


Fig.3. Waveforms.









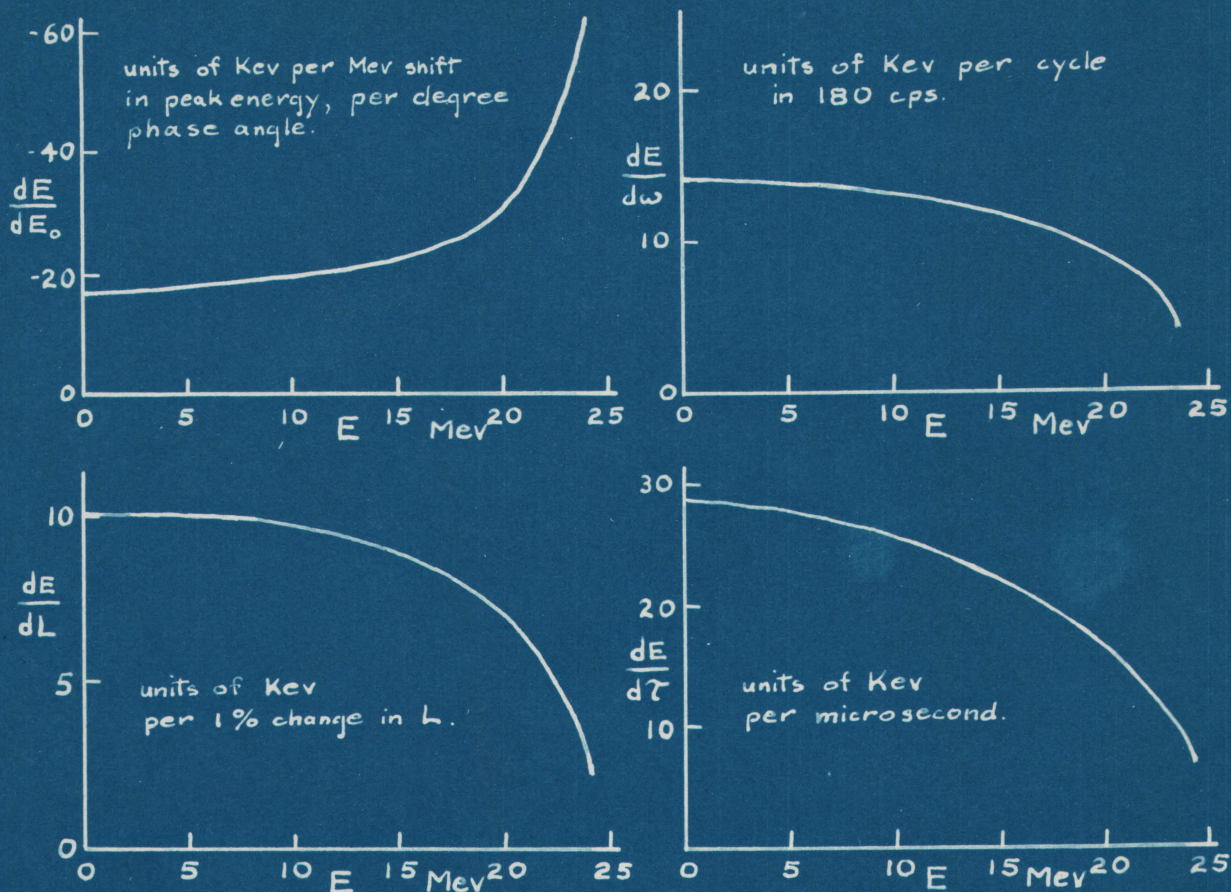


Fig. 5. X-ray Energy Dependences. Magnet Energy 25 Mev.

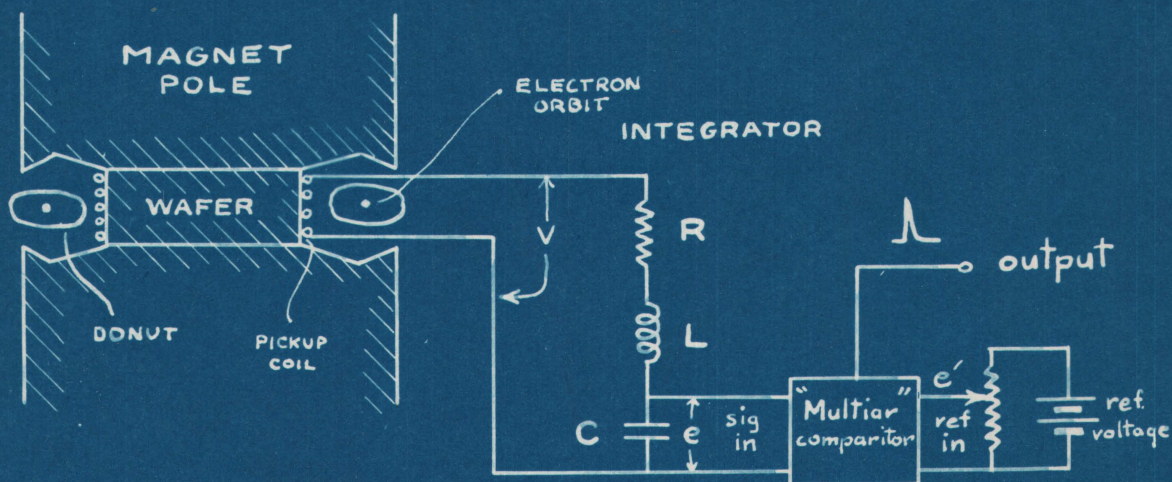


Fig. 6. Schematic Diagram of Pickup Coil and Integrator.